

# Phase-precipitation studies of Fe–B–Si metallic glasses using Mössbauer spectroscopy

N. BANERJI, U. C. JOHRI, V. N. KULKARNI, R. M. SINGRU  
*Department of Physics, Indian Institute of Technology, Kanpur 208016, India*

Phase-precipitation studies have been performed on samples of the metallic glasses  $\text{Fe}_{79}\text{B}_{16}\text{Si}_5$  and  $\text{Fe}_{78}\text{B}_{13}\text{Si}_9$ , heated in the range 300–475 °C for various times (1–16 h) using  $^{57}\text{Fe}$  Mössbauer transmission spectroscopy and X-ray diffraction methods. These measurements have helped in identifying the temperature ranges and annealing durations in which the amorphous structure of these metallic glasses is retained. The results revealed that the thermal stability increases as boron is replaced by silicon in the Fe–B–Si metallic glasses and that these alloys remain amorphous below 450 °C. The various phases precipitated above this temperature were identified as  $\alpha\text{-Fe}$ ,  $\alpha\text{-(Fe, Si)}$ ,  $\text{Fe}_3\text{B}$ , and  $\text{Fe}_2\text{B}$ . The direction of magnetization in the two metallic glasses appears to change upon annealing.

## 1. Introduction

The metallic glasses of the Fe–B–Si system are important for technical applications because they are soft ferromagnetic amorphous alloys having a well-known ability to provide low losses at high frequencies [1–4]. This property is a result of the atomic structure which is amorphous in nature. The atomic structure and, therefore, the physical properties of these amorphous alloys, are very sensitive to the nature of heat treatment given. Upon annealing, the metallic glasses tend to relax and become denser by atomic rearrangement which is controlled by the diffusion of the atoms through the amorphous structure [5]. In view of this, knowledge of the diffusion process in amorphous alloys is important and, therefore, we have studied in our laboratory the diffusion of germanium, palladium, silver and gold atoms in amorphous samples of the metallic glasses  $\text{Fe}_{79}\text{B}_{16}\text{Si}_5$  and  $\text{Fe}_{78}\text{B}_{13}\text{Si}_9$  using the technique of Rutherford backscattering spectrometry [6]. However, the diffusion studies must be carried out at temperatures and for times during which the glassy alloys retain their amorphous structure. It is, therefore, essential to gain knowledge of the kinetics of crystallization so that proper annealing temperatures and times can be selected for studying the diffusion of different species in metallic glasses. With this aim in mind we have investigated the crystallization kinetics of the metallic glasses  $\text{Fe}_{79}\text{B}_{16}\text{Si}_5$  and  $\text{Fe}_{78}\text{B}_{13}\text{Si}_9$  in the temperature range 300–475 °C (for times ranging from 1–16 h) using X-ray diffraction (XRD) and Mössbauer transmission spectroscopy (TMS) techniques. The present studies have thus helped to determine the range of annealing temperatures and times for which the amorphous structure is maintained in these glasses. Generally, Mössbauer spectroscopic studies of metallic glasses have been performed at different temperatures ranging from below room temperature (RT) to temperatures well above its crystallization

temperature,  $T_x$ , and not much work involving room-temperature measurements has been reported to provide a detailed understanding of the effect of annealing for different times below  $T = T_x$ . The present results provide useful information for the metallic glasses heated in the temperature range 300–475 °C for 1–16 h and complement the information obtained from diffusion studies. The results obtained from Rutherford backscattering studies will be reported elsewhere [7] and only the results obtained by X-ray diffraction and Mössbauer spectroscopy will be presented here.

## 2. Experimental procedure

The metallic glasses studied, namely  $\text{Fe}_{79}\text{B}_{16}\text{Si}_5$  (Si5) and  $\text{Fe}_{78}\text{B}_{13}\text{Si}_9$  (Si9), were obtained in the form of thin ribbons (thickness 0.025 mm) from Goodfellow Metals Ltd, Cambridge, UK. Samples of dimensions 8 mm × 10 mm were cut from these ribbons and placed on copper holders to prepare Mössbauer absorbers. These samples were then annealed isothermally in a clean and high vacuum ( $< 1 \times 10^{-5}$  mbar) for several time intervals ranging from 1–16 h at different annealing temperatures (using a separate sample at each temperature) in the range 300–475 °C. The schedule of heat treatment given to each metallic glass sample is described in Tables I and II. The technical data provided by the suppliers [8] listed the crystallization temperature,  $T_x$ , for the Si5 and Si9 glasses as 505 and 550 °C, respectively. The highest temperature (i.e. 475 °C) used in the present annealing process was, therefore, below  $T_x$  of each glass. Mössbauer transmission spectra of the samples were recorded at room temperature (RT = 295 K) before annealing (i.e. as-received samples) and after each heat treatment. The Mössbauer spectrometer, coupled to a multichannel analyser (MCA) was operated in the

constant acceleration mode using a  $^{57}\text{Co}$  source embedded in rhodium matrix (Amersham International Limited, Amersham, UK), and was calibrated with a standard  $\alpha\text{-Fe}$  foil. To obtain Mössbauer parameters, the observed Mössbauer spectra were analysed using a least-squares fitting computer program employing Lorentzian shapes for the peaks. The X-ray diffraction spectra were recorded using an X-ray powder diffractometer (Rich-Seifert Iso-Debyeflex 2002), with a  $\text{CrK}_\alpha$  source.

### 3. Results and discussion

#### 3.1. X-ray analysis of $\text{Fe}_{79}\text{B}_{16}\text{Si}_5$ and $\text{Fe}_{78}\text{B}_{13}\text{Si}_9$

The X-ray diffraction patterns were observed for the metallic glass samples Si5 and Si9, in the as-received form and after different heat treatments (see Tables I and II), and some of these spectra are shown in Fig. 1. The as-received samples show a broad but shallow maximum characteristic of amorphous alloys. With the rise in annealing temperature, the peaks describing

the maximum become sharper but there is no indication of precipitation of any crystalline phase up to the annealing temperature of  $400^\circ\text{C}$ .

In the case of Si5 alloy (Fig. 1), the X-ray diffraction pattern for the annealing temperature of  $450^\circ\text{C}$  (4 h) indicates an onset of crystallization. Other workers [9–16] have found that crystalline phases corresponding to  $\text{Fe}_3\text{B}$ ,  $\alpha\text{-(Fe, Si)}$  or  $\text{Fe}_3\text{Si}$  and  $\text{Fe}_2\text{B}$  could be identified during the crystallization of the Fe–B–Si alloys. The actual mode of crystallization appears to depend on the particular composition of the Fe–B–Si alloy. In particular, the formation of the metastable  $\text{Fe}_3\text{B}$  phase is related to the formation of iron–silicon phase which is produced during the first stages of crystallization [10]. In the case of alloys having low silicon content (Si/B ratio  $< 1$ ) the formation of the  $\text{Fe}_3\text{B}$  and  $\alpha\text{-(Fe, Si)}$  phases appears favourable [10]. Formation of a substitutional solid solution  $\alpha\text{-(Fe, Si)}$ , in which the silicon atoms occupy the sites of the iron atoms in the  $\alpha\text{-Fe}$  (b c c) structure [10] has been clearly observed by several workers [9, 11, 15, 16]. The lattice parameter of  $\alpha\text{-(Fe, Si)}$  is slightly less

TABLE I Details of heat treatment given to the Si5 metallic glass ( $\text{Fe}_{79}\text{B}_{16}\text{Si}_5$ ) and the Mössbauer parameters obtained from computer analysis of the present data. The assignments proposed on the basis of Mössbauer spectroscopic and X-ray diffraction (XRD) data are listed in the last column

Annealing temp. ( $^\circ\text{C}$ )	Annealing time (h)	IS <sup>a</sup> ( $\text{mm s}^{-1}$ )	$H^b$ kOe	$\Gamma^c$ ( $\text{mm s}^{-1}$ )	Assignment	
					Mössbauer	XRD <sup>d</sup>
300	1	0.10	242	1.09	Amorphous	Amorphous
	4	0.03	243	1.21	Amorphous	Amorphous
	8	0.10	239	1.01	Amorphous	Amorphous
	16	0.10	240	1.04	Amorphous	Amorphous
350	1	0.01	237	1.00	Amorphous	Amorphous
	2	0.05	239	1.08	Amorphous	Amorphous
	4	0.05	238	1.00	Amorphous	Amorphous
	8	0.03	240	1.07	Amorphous	Amorphous
	16	0.01	239	1.04	Amorphous	Amorphous
400	1	0.02	240	1.05	Amorphous	Amorphous
	2	0.01	239	1.08	Amorphous	Amorphous
	4	0.02	239	1.05	Amorphous	Amorphous
	8	0.02	240	1.05	Amorphous	Amorphous
	16	0.01	239	1.07	Amorphous	Amorphous
450	1	0.01	242	1.17	Amorphous	Amorphous
450	4	(1) 0.00	334	0.29	$\alpha\text{-Fe}$	$\alpha\text{-Fe}$
		(2) 0.03	331	0.49	Fe–Si (8 nn)	N.O.
		(3) 0.08	311	0.39	Fe–Si (7 nn)	N.O.
		(4) 0.02	288	0.39	Fe–Si (6 nn)	N.O.
		(5) 0.07	268	0.49	t- $\text{Fe}_3\text{B}$	N.O.
		(6) 0.09	247	0.43	t- $\text{Fe}_3\text{B}$	N.O.
		(7) 0.11	229	0.40	Fe–Si (5 nn)	N.O.
		(8) 0.08	200	0.49	$\text{Fe}_2\text{B}$ (avg)	N.O.
		(9) 0.11	229	0.40	t- $\text{Fe}_3\text{B}$	N.O.
		(10) 0.08	200	0.49	Fe–Si (4 nn)	N.O.
		(11) 0.08	200	0.49	Fe–Si (4 nn)	N.O.
450	8	(1) 0.00	334	0.29	$\alpha\text{-Fe}$	$\alpha\text{-Fe}$
		(2) 0.03	331	0.51	Fe–Si (8 nn)	N.O.
		(3) 0.08	311	0.39	Fe–Si (7 nn)	N.O.
		(4) 0.02	288	0.39	Fe–Si (6 nn)	N.O.
		(5) 0.07	268	0.49	t- $\text{Fe}_3\text{B}$	N.O.
		(6) 0.09	247	0.39	t- $\text{Fe}_3\text{B}$	N.O.
		(7) 0.11	229	0.39	Fe–Si (5 nn)	N.O.
		(8) 0.08	200	0.49	$\text{Fe}_2\text{B}$ (avg)	N.O.
		(9) 0.11	229	0.39	t- $\text{Fe}_3\text{B}$	N.O.
		(10) 0.08	200	0.49	Fe–Si (4 nn)	N.O.
		(11) 0.08	200	0.49	Fe–Si (4 nn)	N.O.

TABLE I (Continued)

Annealing temp. (°C)	Annealing time (h)	IS <sup>a</sup> (mm s <sup>-1</sup> )	H <sup>b</sup> (kOe)	Γ <sup>c</sup> (mm s <sup>-1</sup> )	Assignment	
					Mössbauer	XRD <sup>d</sup>
450	16	(1) 0.00	334	0.29	α-Fe	α-Fe
		(2) 0.03	331	0.43	Fe-Si (8 nn)	N.O.
		(3) 0.06	313	0.43	Fe-Si (7 nn)	N.O.
		(4) 0.18	283	0.45	Fe-Si (6 nn)	N.O.
					t-Fe <sub>3</sub> B	N.O.
		(5) 0.07	268	0.39	t-Fe <sub>3</sub> B	N.O.
		(6) 0.24	238	0.39	Fe-Si (5 nn)	N.O.
					Fe <sub>2</sub> B (avg)	N.O.
			Fe <sub>3</sub> B	N.O.		
			Fe-Si (4 nn)	N.O.		
475	1	(1) 0.14	334	0.29	α-Fe	α-Fe
		(2) 0.03	327	0.39	Fe-Si (8 nn)	N.O.
		(3) 0.12	311	0.39	Fe-Si (7 nn)	N.O.
		(4) 0.11	288	0.39	Fe-Si (6 nn)	N.O.
					t-Fe <sub>3</sub> B	Fe <sub>3</sub> B
		(5) 0.07	266	0.43	t-Fe <sub>3</sub> B	Fe <sub>3</sub> B
		(6) 0.08	242	0.43	Fe-Si (5 nn)	N.O.
					Fe <sub>2</sub> B (avg)	Fe <sub>2</sub> B
			t-Fe <sub>3</sub> B	Fe <sub>3</sub> B		
			Fe-Si (4 nn)	N.O.		
475	2	(1) 0.07	331	0.30	α-Fe	α-Fe
		(2) 0.11	327	0.48	Fe-Si (8 nn)	N.O.
		(3) 0.14	310	0.33	Fe-Si (7 nn)	N.O.
		(4) 0.21	286	0.30	Fe-Si (6 nn)	N.O.
					t-Fe <sub>3</sub> B	Fe <sub>3</sub> B
		(5) 0.27	269	0.54	t-Fe <sub>3</sub> B	Fe <sub>3</sub> B
		(6) 0.16	239	0.42	Fe-Si (5 nn)	N.O.
					Fe <sub>2</sub> B (avg)	Fe <sub>2</sub> B
			t-Fe <sub>3</sub> B	Fe <sub>3</sub> B		
			FeSi (4 nn)	N.O.		
475	4	(1) -0.02	334	0.30	α-Fe	α-Fe
		(2) 0.08	327	0.40	Fe-Si (8 nn)	N.O.
		(3) 0.04	311	0.40	Fe-Si (7 nn)	N.O.
		(4) 0.08	288	0.40	Fe-Si (6 nn)	N.O.
					t-Fe <sub>3</sub> B	Fe <sub>3</sub> B
		(5) 0.01	269	0.40	t-Fe <sub>3</sub> B	Fe <sub>3</sub> B
		(6) 0.14	239	0.40	Fe-Si (5 nn)	N.O.
					Fe <sub>2</sub> B (avg)	Fe <sub>2</sub> B
			t-Fe <sub>3</sub> B	Fe <sub>3</sub> B		
			Fe-Si (4 nn)	N.O.		
475	6	(1) -0.03	335	0.38	α-Fe	α-Fe
		(2) 0.10	329	0.40	Fe-Si (8 nn)	N.O.
		(3) 0.03	311	0.32	Fe-Si (7 nn)	N.O.
		(4) 0.15	290	0.48	Fe-Si (6 nn)	N.O.
					t-Fe <sub>3</sub> B	Fe <sub>3</sub> B
		(5) -0.02	263	0.40	t-Fe <sub>3</sub> B	Fe <sub>3</sub> B
		(6) 0.10	235	0.32	Fe-Si (5 nn)	N.O.
					Fe <sub>2</sub> B (avg)	Fe <sub>2</sub> B
			t-Fe <sub>3</sub> B	Fe <sub>3</sub> B		
			Fe-Si (4 nn)	N.O.		
475	8	(1) 0.08	334	0.29	α-Fe	α-Fe
		(2) 0.10	329	0.31	Fe-Si (8 nn)	N.O.
		(3) 0.13	313	0.41	Fe-Si (7 nn)	N.O.
		(4) 0.24	286	0.34	Fe-Si (6 nn)	N.O.
					t-Fe <sub>3</sub> B	Fe <sub>3</sub> B
		(5) 0.25	265	0.30	t-Fe <sub>3</sub> B	Fe <sub>3</sub> B
		(6) 0.20	238	0.31	Fe-Si (5 nn)	N.O.
					Fe <sub>2</sub> B (avg)	Fe <sub>2</sub> B
			t-Fe <sub>3</sub> B	Fe <sub>3</sub> B		
			Fe-Si (4 nn)	N.O.		

<sup>a</sup> Isomer shift measured with respect to α-Fe: typical error ± 0.01.

<sup>b</sup> Internal magnetic field at <sup>57</sup>-Fe nucleus: typical error ± 5.00.

<sup>c</sup> Width of the spectral line: typical error ± 0.01.

<sup>d</sup> N.O. = Not observed.

TABLE II Details of heat treatment given to the Si9 metallic glass ( $\text{Fe}_{78}\text{B}_{13}\text{Si}_9$ ) and the Mössbauer parameters obtained from computer analysis of the present data. The assignments proposed on the basis of Mössbauer spectroscopic and X-ray diffraction (XRD) data are listed in the last column

Annealing temp. (°C)	Annealing time (h)	IS <sup>a</sup> (mm s <sup>-1</sup> )	H <sup>b</sup> kOe	$\Gamma^d$ (mm s <sup>-1</sup> )	Assignment	
					Mössbauer	XRD <sup>d</sup>
300	1	0.12	252	0.94	Amorphous	Amorphous
	4	0.01	255	0.97	Amorphous	Amorphous
	8	0.14	252	0.91	Amorphous	Amorphous
	16	0.12	254	0.91	Amorphous	Amorphous
350	1	0.03	250	0.90	Amorphous	Amorphous
	2	0.06	252	0.96	Amorphous	Amorphous
	4	0.05	253	0.91	Amorphous	Amorphous
	8	0.04	254	0.90	Amorphous	Amorphous
	16	0.04	254	0.93	Amorphous	Amorphous
400	1	0.04	252	0.93	Amorphous	Amorphous
	2	0.07	254	1.01	Amorphous	Amorphous
	4	0.04	251	0.98	Amorphous	Amorphous
	8	0.06	255	0.94	Amorphous	Amorphous
	16	0.04	255	0.97	Amorphous	Amorphous
450	1	0.10	261	0.92	Amorphous	Amorphous
	4	0.12	258	1.06	Amorphous	Amorphous
	8	0.22	255	1.29	Amorphous	Amorphous
	16	0.19	253	1.12	Amorphous	Amorphous
475	1	(1) 0.13	334	0.29	$\alpha$ -Fe	$\alpha$ -Fe
		(2) 0.18	331	0.29	Fe-Si (8 nn)	N.O.
		(3) 0.28	314	0.45	Fe-Si (7 nn)	N.O.
		(4) 0.15	286	0.45	Fe-Si (6 nn)	N.O.
		(5) 0.17	266	0.43	t-Fe <sub>3</sub> B (avg)	N.O.
		(6) 0.16	250	0.64	Fe-Si (5 nn)	N.O.
		(7) 0.22	235	0.57	Fe <sub>2</sub> B (avg)	N.O.
		(8) 0.11	203	0.68	Fe-Si (4 nn)	N.O.
475	2	(1) 0.13	334	0.58	$\alpha$ -Fe	$\alpha$ -Fe
		(2) 0.18	331	0.58	Fe-Si (8 nn)	N.O.
		(3) 0.28	314	0.78	Fe-Si (7 nn)	N.O.
		(4) 0.15	286	0.86	Fe-Si (6 nn)	N.O.
		(5) 0.17	266	0.86	t-Fe <sub>3</sub> B (avg)	Fe <sub>3</sub> B
		(6) 0.16	250	1.15	Fe-Si (5 nn)	N.O.
		(7) 0.22	235	1.14	Fe <sub>2</sub> B (avg)	Fe <sub>2</sub> B
		(8) 0.11	203	1.36	Fe-Si (4 nn)	N.O.
475	4	(1) 0.08	334	0.58	$\alpha$ -Fe	$\alpha$ -Fe
		(2) 0.13	331	0.58	Fe-Si (8 nn)	N.O.
		(3) 0.08	309	0.58	Fe-Si (7 nn)	N.O.
		(4) 0.07	286	0.58	Fe-Si (6 nn)	N.O.
		(5) 0.06	267	0.78	t-Fe <sub>3</sub> B (avg)	Fe <sub>3</sub> B
		(6) 0.05	253	1.10	Fe-Si (5 nn)	N.O.
		(7) 0.06	235	1.14	Fe <sub>2</sub> B (avg)	Fe <sub>2</sub> B
		(8) 0.01	203	1.44	Fe-Si (4 nn)	N.O.
475	6	(1) 0.08	334	0.58	$\alpha$ -Fe	$\alpha$ -Fe
		(2) 0.13	331	0.58	Fe-Si (8 nn)	N.O.
		(3) 0.06	318	0.91	Fe-Si (7 nn)	N.O.
		(4) 0.08	289	0.90	Fe-Si (6 nn)	N.O.
		(5) 0.02	265	0.78	t-Fe <sub>3</sub> B (avg)	Fe <sub>3</sub> B
		(6) 0.22	242	0.78	Fe-Si (5 nn)	N.O.
		(7) 0.11	235	0.72	Fe <sub>2</sub> B (avg)	Fe <sub>2</sub> B
		(8) 0.29	196	0.78	Fe-Si (4 nn)	N.O.
475	8	(1) 0.09	334	0.58	$\alpha$ -Fe	$\alpha$ -Fe
		(2) 0.15	330	0.58	Fe-Si (8 nn)	N.O.
		(3) 0.13	314	0.78	Fe-Si (7 nn)	N.O.
		(4) 0.11	286	0.78	Fe-Si (6 nn)	N.O.
		(5) 0.07	268	0.72	t-Fe <sub>3</sub> B (avg)	Fe <sub>3</sub> B
		(6) 0.25	243	0.78	Fe-Si (5 nn)	N.O.
		(7) 0.11	235	0.72	Fe <sub>2</sub> B (avg)	Fe <sub>2</sub> B
		(8) 0.20	196	0.78	Fe-Si (4 nn)	N.O.

<sup>a</sup> Isomer shift measured with respect to  $\alpha$ -Fe: typical error  $\pm 0.01$ .

<sup>b</sup> Internal magnetic field at <sup>57</sup>Fe nucleus: typical error  $\pm 5.00$ .

<sup>c</sup> Width of the spectral line: typical error  $\pm 0.01$ .

<sup>d</sup> N.O. = Not observed.

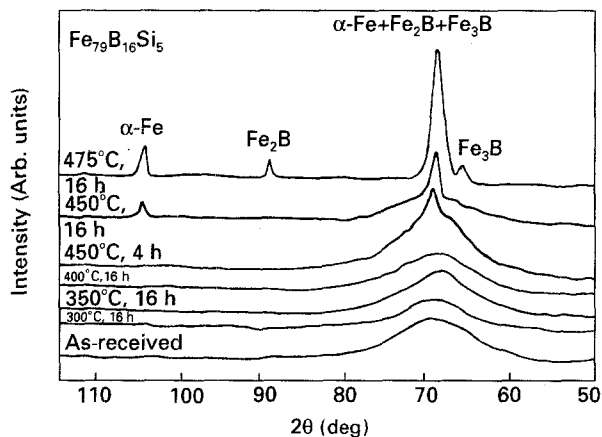


Figure 1 X-ray diffraction pattern (at RT) of Si5, heat treated at various temperatures for 16 h.

than that for  $\alpha$ -Fe and this causes the X-ray diffraction peak of  $\alpha$ -(Fe, Si) to occur at slightly higher value of  $2\theta$  compared to  $\alpha$ -Fe [10]. Using this information in the analysis of Fig. 1, we conclude that the crystalline phases of  $\alpha$ -(Fe, Si) and  $\text{Fe}_2\text{B}$  were precipitated in the Si5 sample annealed at  $475^\circ\text{C}$  for 16 h. However, the presence of the  $\text{Fe}_3\text{B}$  phase is not unambiguously indicated in the X-ray diffraction pattern because the peaks due to t- $\text{Fe}_3\text{B}$  and t- $\text{Fe}_2\text{B}$  overlap around  $2\theta$  equal to  $66^\circ$  and  $69^\circ$ . The peak due to t- $\text{Fe}_3\text{B}$  is also expected at  $2\theta$  equal to  $75.04^\circ$ , but it is not observed in Fig. 1. The present Mössbauer spectroscopic studies of the Si5 sample, however, indicate the presence of t- $\text{Fe}_3\text{B}$  phase for samples annealed at  $450^\circ\text{C}$  for 4 h and at higher temperatures. This discrepancy between the two measurements will be discussed later.

In the case of the Si9 sample, the presence of crystallized phases is not indicated even for an annealing temperature of  $450^\circ\text{C}$  (16 h), but becomes clear for the sample heat treated at  $475^\circ\text{C}$  (16 h). This difference in the behaviour of the Si5 and Si9 alloys is ascribed to the higher concentration of silicon in Si9 which leads to an improved thermal stability of the Si9 alloy [16, 17]. The analysis of the X-ray diffraction pattern for the Si9 sample annealed at  $475^\circ\text{C}$  (16 h) indicates the presence of  $\alpha$ -(Fe, Si), t- $\text{Fe}_2\text{B}$  and perhaps t- $\text{Fe}_3\text{B}$ .

The present results obtained by X-ray diffraction studies compare well with those reported by other workers. Ramanan and Fish [9] have observed the crystallization of  $\alpha$ -(Fe, Si) and  $\text{Fe}_3\text{B}$  in the Fe-B-Si alloys. The studies reported by Quivy *et al.* [12] indicate the precipitation of the  $\alpha$ -(Fe-Si) and  $\text{Fe}_3\text{B}$  phases in samples of  $\text{Fe}_{79}\text{B}_{16}\text{Si}_5$  when annealed at  $475^\circ\text{C}$  (30 min) and in samples of  $\text{Fe}_{78}\text{B}_{13}\text{Si}_9$  when annealed at  $495^\circ\text{C}$  (30 min). In the case of the  $\text{Fe}_{78}\text{B}_{13}\text{Si}_9$  alloy, the X-ray diffraction studies of Bang and Lee [15] revealed that the crystallization occurred in two stages. In the first stage (occurring at  $450^\circ\text{C}$ )  $\alpha$ -(Fe, Si) and metastable  $\text{Fe}_3\text{B}$  were formed. Further heating up to  $550^\circ\text{C}$  lead to the decomposition of the metastable  $\text{Fe}_3\text{B}$  into the stable phase  $\text{Fe}_2\text{B}$  together with  $\alpha$ -Fe. It should be pointed out that the  $\text{Fe}_3\text{B}$  phase has been observed only for few glasses of the Fe-B-Si alloys [9, 12, 15]. These differences are ascribed to the sensitive role played by the relative

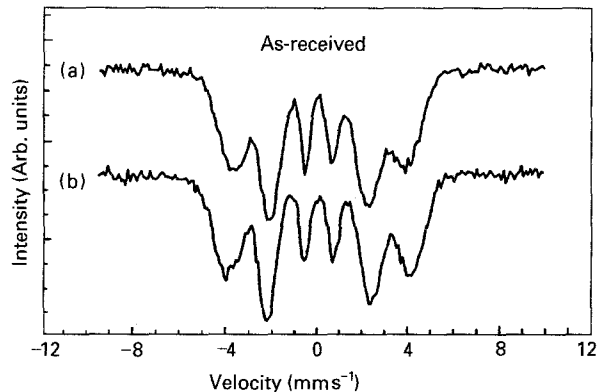


Figure 2 Mössbauer (RT) spectra of as-received (a) Si5 and (b) Si9 samples.

concentration of metalloids in determining the crystallization temperature and formation of different phases. In addition, different samples of the same alloy composition are prepared with different manufacturing methods involving different quenching rates and hence result in different quenched-in nuclei.

## 3.2. Mössbauer spectroscopic studies

### 3.2.1. Study of as-received samples of Si5 and Si9

The Mössbauer spectra for the Si5 and Si9 samples, in the as-received form and recorded at room temperature are shown in Fig. 2. They display well-defined but broadened lines and it is well known that such broadening is characteristic of amorphous magnetic solids. These spectra were analysed with a computer program and these results indicate that the isomer shift (IS) increases from  $0.06 \pm 0.01 \text{ mm s}^{-1}$  to  $0.08 \pm 0.01 \text{ mm s}^{-1}$  as the concentration of silicon is raised from 5% to 9%. Similar observations have been made for other Fe-B-Si metallic glasses by Taniwaki and Maida [18] and Singhal *et al.* [16]. A possible explanation for such an increase of IS with silicon concentration was also given in our earlier report [16]. The present results for the internal magnetic field,  $H$ , for the as-received samples show that  $H$  increases from 235 kOe (for 5 at % Si) to 247 kOe (for 9 at % Si). Similar increase in  $H$  with increasing silicon concentration has been reported in the literature [18–20]. This behaviour has been ascribed to the strain caused during the replacement of a small metalloid (boron) by a larger metalloid (silicon) atom in the interstitial site. We further observe that the full width at half maximum,  $\Gamma$ , of the spectral lines decrease from  $1.12 \pm 0.01 \text{ mm s}^{-1}$  for Si5 to  $0.94 \pm 0.01 \text{ mm s}^{-1}$  for Si9 (Table I). A similar behaviour is shown by the  $\text{Fe}_{80}\text{B}_{20-x}\text{Si}_x$  metallic glasses where  $\Gamma$  was observed to decrease from  $0.92 \pm 0.01 \text{ mm s}^{-1}$  to  $0.86 \pm 0.01 \text{ mm s}^{-1}$  as  $x$  was increased from 0 to 8.

### 3.2.2. Study of heat-treated samples

3.2.2.1.  $\text{Fe}_{79}\text{B}_{16}\text{Si}_5$  (or Si5). As mentioned earlier, samples of Si5 were heated at various temperatures for different time periods as described in Table I, and their

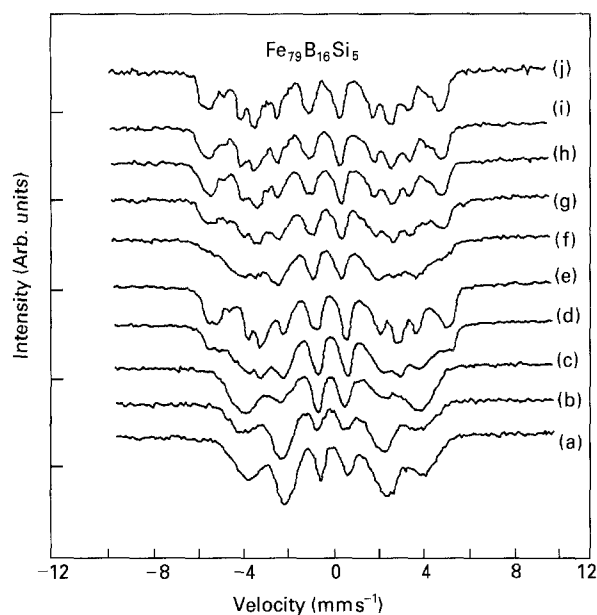


Figure 3 Mössbauer (RT) spectra of Si5 sample, annealed at the given temperatures and times: (a) 300°C, 16 h; (b) 350°C, 16 h; (c) 400°C, 16 h; (d) 450°C, 8 h; (e) 450°C, 16 h; (f) 475°C, 1 h; (g) 475°C, 2 h; (h) 475°C, 4 h; (i) 475°C, 6 h; (j) 475°C, 8 h.

Mössbauer transmission spectra were recorded at room temperature. Some of these spectra are shown in Fig. 3 and the resulting Mössbauer parameters are given in Table I. It was observed that the samples of Si5 heat treated at (i) 300°C for 1, 4, 8, and 16 h, (ii) 350°C for 1, 2, 4, and 8 h, and (iii) 400°C for 1, 4, and 8 h, show Mössbauer spectra whose shape is similar to the six-finger pattern (with broad lines) shown by the as-received sample. This behaviour suggests that the samples of Si5 heat treated at these temperatures (for the given times) retain their amorphous nature. As discussed in Section 3.1, this conclusion is also supported by the X-ray diffraction studies. Heat treatment given to the Si5 alloy at 400°C for 16 h appears to usher changes in the nature of the Mössbauer spectrum and these changes (Fig. 3) appear to develop quickly as the sample is heat treated at 450°C

for 1, 4, 8, and 16 h. The broad six-finger pattern of Mössbauer spectrum changes into a more complicated spectrum composed of several lines, and this behaviour indicates the onset of crystallization process in the metallic glass  $\text{Fe}_{79}\text{B}_{16}\text{Si}_5$ . By the time the sample is heat treated for 2 h at 475°C, the crystallization process appears to have advanced and has perhaps progressed further when the heat treatment was carried out at 475°C at 8 h (Fig. 3).

It has been reported earlier [9–16] that the crystallization process of the Si5 glass gives rise to different phases of  $t\text{-Fe}_3\text{B}$ ,  $\text{Fe}_2\text{B}$ ,  $\alpha\text{-Fe}$ , and  $\text{Fe-Si}$ . The computer analysis of the Mössbauer spectra observed by us required the knowledge of  $H$  for these phases to obtain a best fit. The values of  $H$  used by us for obtaining such a fit are given in Table III, and they were compiled from the values reported in the literature [14, 21–25].

The Mössbauer spectra observed for the samples heated at 450°C (16 h) and above appeared complicated and they were fitted into seven subspectra. In order to provide an idea about the computer fit, we have shown in Fig. 4 the Mössbauer spectra of the Si5 sample heat treated at 475°C for 8 h and fitted into seven subspectra. The values of the Mössbauer parameters obtained for these subspectra are listed in Table I. The analysis indicates the formation of the phases  $\alpha\text{-Fe}$ ,  $\text{Fe}_3\text{B}$ ,  $\text{Fe}_2\text{B}$ , and  $\alpha\text{-(Fe, Si)}$ . Sanchez *et al.* [21] have found evidence for a mixture of tetragonal and orthorhombic  $\text{Fe}_3\text{B}$  phase in the heat-treated samples of  $\text{Fe}_{100-x}\text{B}_x$  glasses. The tetragonal phase (t) of  $\text{Fe}_3\text{B}$  appears to have been formed at three iron sites, while  $\text{Fe}_2\text{B}$  is observed to give only one value of  $H$ . Actually, Takacs *et al.* [22] have obtained  $H$  values corresponding to two iron sites ( $H = 242.0$  and  $231.7$  kOe) in  $\text{Fe}_2\text{B}$ . These two values of  $H$  are quite close and it appears that our measurement has not been able to resolve them and we have thus observed an average value. This averaging is ascribed to the effect of the broad lines (arising out of the incomplete crystallization) and interference from the  $\alpha\text{-(Fe, Si)}$

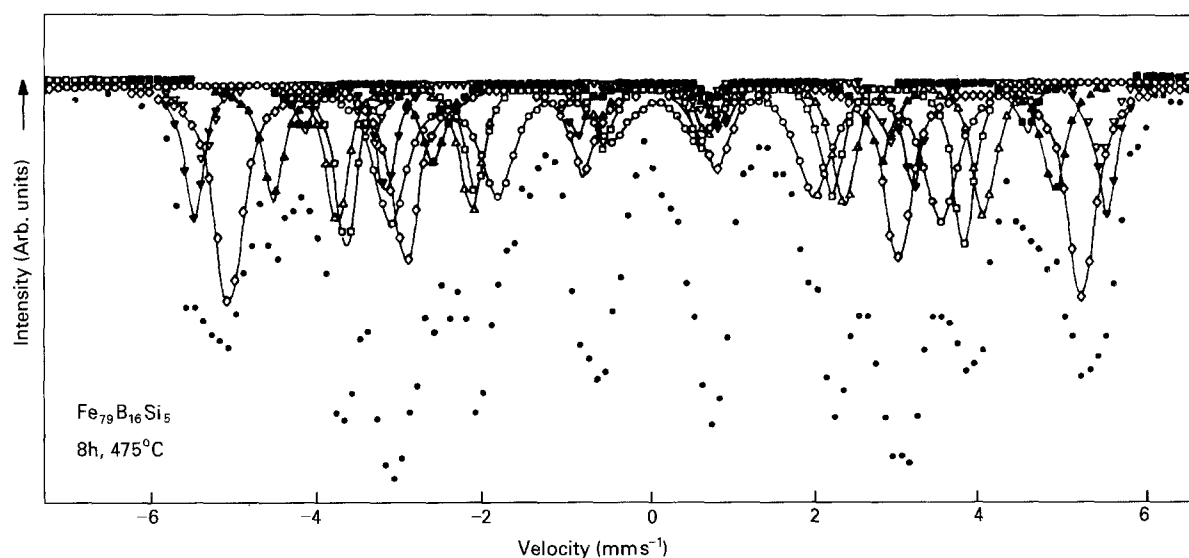


Figure 4 Analysed form of Mössbauer spectrum (RT) of a heat treated sample of Si5 indicating the various phases precipitated: (▼)  $\alpha\text{-Fe}$ , (▽)  $\text{Fe-Si}(8\text{nn})$ , (◇)  $\text{Fe-Si}(7\text{nn})$ , (▲)  $\text{Fe-Si}(6\text{nn})$ , (■)  $t\text{-Fe}_3\text{B}(\text{avg})$ , (△)  $\text{Fe-Si}(5\text{nn})$ , (□)  $t\text{-Fe}_2\text{B}(\text{avg})$ , (○)  $\text{Fe-Si}(4\text{nn})$ .

TABLE III Reported values of internal magnetic field,  $H$ , of magnetic phases observed in the crystallization of the Fe-B-Si metallic glasses

Phase observed	Site	$H$ (kOe)	Reference
$\alpha$ -Fe		330	[21]
t-Fe <sub>2</sub> B	1	232	[22]
	2	242	
	avg	237	
t-Fe <sub>3</sub> B	1	226	[23]
	2	265	
	3	288	
	avg	259	
Fe-8.6 at % Si (b c c)	8 nn	331	[24]
	7 nn	308	
	6 nn	277	
Fe-18.1 at % Si (b c c)	8 nn	325	[25]
	7 nn	306	
	6 nn	284	
	5 nn	244	
	4 nn	192	
Fe-14.8 at % Si (b c c)	8 nn	328	[14]
	7 nn	313	
	6 nn	285	
	5 nn	239	
	4 nn	201	

lines. Previous work [14, 24] has shown that silicon in the  $\alpha$ -(Fe, Si) solid solution is situated at different nearest neighbour (nn) iron atom sites. Because the values of  $H$  in  $\alpha$ -(Fe, Si) solid solution are expected to depend on the nearest neighbour distributions, we have fitted the  $H$  values by using the observed values of  $H$  for 8, 7, 6, 5 and 4 nearest neighbour iron atom sites in  $\alpha$ -(Fe, Si) (Table III). The Fe<sub>3</sub>B phase is known to be metastable and at higher temperatures it decomposes according to Fe<sub>3</sub>B  $\rightarrow$  Fe<sub>2</sub>B +  $\alpha$ -Fe [26, 27]. Because the present heat treatment was carried out at  $T \leq 475^\circ\text{C}$ , the crystallization temperature ( $T_x = 515^\circ\text{C}$ ) was not reached and the decomposition of Fe<sub>3</sub>B into Fe<sub>2</sub>B and  $\alpha$ -Fe was perhaps not complete. Therefore, we expect the presence of Fe<sub>3</sub>B, Fe<sub>2</sub>B and  $\alpha$ -Fe phases in our samples, and this conclusion is supported by our results (Table I). It should be pointed out that the presence of the Fe<sub>3</sub>B phase in our samples is brought out more clearly by the results of Mössbauer spectroscopy than by the X-ray diffraction patterns. This difference can be attributed to the different sensitivities of the two methods. Quivy *et al.* [12] have observed the formation of  $\alpha$ -Fe and Fe<sub>3</sub>B phases in metallic glass Fe<sub>79</sub>B<sub>16</sub>Si<sub>5</sub> (heat treated at 475°C for 30 min) by X-ray diffraction and transmission electron microscopic techniques. Mössbauer spectroscopic studies of Fe<sub>83</sub>B<sub>12</sub>Si<sub>5</sub> [28] have shown that above 500°C, the products of crystallization were  $\alpha$ -Fe, Fe<sub>2</sub>B, and  $\alpha$ -(Fe, Si). Similarly, studies by Ok and Morrish [29] using Mössbauer spectroscopy, X-ray diffraction and density measurements showed that the heat treatment of Fe<sub>82</sub>B<sub>12</sub>Si<sub>6</sub> gives rise to a transformation involving several stages, with the final products being Fe<sub>2</sub>B and Fe-9 at % Si ( $\alpha$ -Fe being absent).

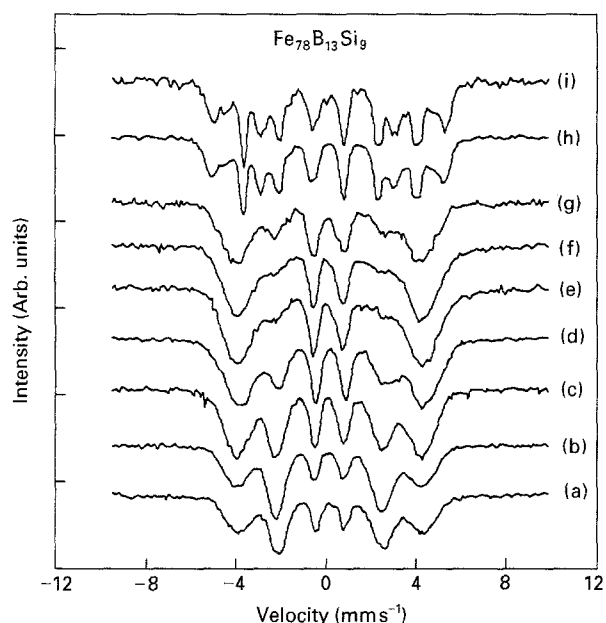


Figure 5 Mössbauer (RT) spectra of Si9 sample, annealed at given temperatures and times: (a) 300°C, 16 h; (b) 350°C, 16 h; (c) 400°C, 16 h; (d) 450°C, 16 h; (e) 475°C, 1 h; (f) 475°C, 2 h; (g) 475°C, 4 h; (h) 475°C, 6 h; (i) 475°C, 8 h.

3.2.2.2. *Fe<sub>78</sub>B<sub>13</sub>Si<sub>9</sub> (or Si9)*. The heat treatment of the as-received samples of Si9 alloy was carried out at different temperatures (and times) as described in Table II. Mössbauer spectra of the samples heat treated at 300, 350 and 400°C (for times ranging from 1–16 h) are shown in Fig. 5, and they consist of six broad lines (having  $\Gamma$  ranging from  $0.9 \pm 0.01$  to  $1.0 \pm 0.01 \text{ mm s}^{-1}$ ) which are typical of the amorphous phase. It is observed that this behaviour continues for the samples of Si9 heat treated at 450°C for 1, 4, 8, and 16 h. Changes in the shape of the Mössbauer spectra are observed for the samples heat treated at 475°C for 6 and 8 h, thus indicating the onset of crystallization process. These changed spectra were complicated in nature and could be best fitted with the subspectra characteristic of Fe<sub>3</sub>B,  $\alpha$ -Fe, Fe<sub>2</sub>B and  $\alpha$ -(Fe, Si). The values of the Mössbauer parameters and assignment of phases are listed in Table II, and they indicate a general similarity between the two metallic glasses. The present results further indicate that the crystallization of the metallic glass Si9 was not complete even after it was heated at 475°C for 8 h. This result is to be expected because the value of  $T_x$  for the Fe<sub>78</sub>B<sub>13</sub>Si<sub>9</sub> metallic glass, as specified by the supplier, was 550°C. The value of  $T_x$  for the same composition (but samples obtained from other sources), has been reported by Bhatnagar and Ravi [30] to be 563°C and by Nagarajan *et al.* [14] to be 559°C.

### 3.2.3. Comparison between the two metallic glasses Si5 and Si9

At this stage, a brief comparison of the results obtained for Fe<sub>79</sub>B<sub>16</sub>Si<sub>5</sub> and Fe<sub>78</sub>B<sub>13</sub>Si<sub>9</sub> is in order. First, the X-ray diffraction as well as the Mössbauer spectroscopic studies indicate that the higher concentration of silicon has improved the thermal stability of

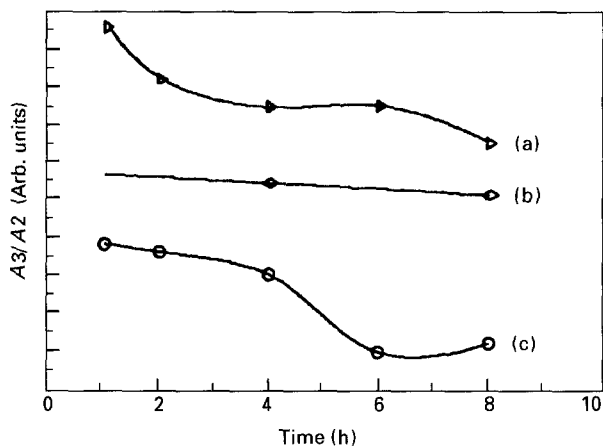


Figure 6 Variation in the ratios of the area under the  $\text{Fe}_3\text{B}$  and  $\text{Fe}_2\text{B}$  sextets obtained from the computer analysis of Mössbauer spectra observed at RT for the following heat treated samples: (a) Si9, 475°C; (b) Si5, 450°C; (c) Si5, 475°C.

these metallic glasses. The two techniques also show a general agreement about the assignment of phases that have crystallized in each glass. In order to gain further insight into the kinetics of crystallization, we determined the ratio,  $A3/A2$ , of the areas under the sextets of  $\text{Fe}_3\text{B}$  and  $\text{Fe}_2\text{B}$  obtained from the computer-fitted Mössbauer spectra. Values of the ratio  $A3/A2$  were determined for the Si5 alloy (heated at 450 and 475°C) and Si9 alloy (heated at 475°C), and their variation with the time period of heat treatment is shown in Fig. 6. These results, indicate that in the case of the Si5 alloy the ratio  $A3/A2$  does not change with  $t$  when the annealing temperature is 450°C. However, the ratio  $A3/A2$  decreases by about 35% over  $t = 8$  h, when the annealing temperature is increased to 475°C. This behaviour indicates that the higher annealing temperature promotes the decomposition  $\text{Fe}_3\text{B} \rightarrow \text{Fe}_2\text{B} + \alpha\text{-Fe}$ , and the amount of decomposition increases with the time period of annealing. In the case of the Si9 alloy, the decrease in the ratio  $A3/A2$  (for the sample heated at 475°C) is slow up to  $t = 4$  h but becomes rapid between 4 and 8 h, with a total decrease of 75% over  $t = 16$  h. This behaviour is understood in terms of the improved thermal stability of the Si9 alloy.

General similarities in the values of Mössbauer parameters obtained at 475°C for the Si5 and Si9 alloys (Tables I and II) indicate that a decrease in the boron content, with an accompanying increase in the silicon content, does not cause large changes as long as the (boron + silicon) content remains approximately same. A minor difference observed by us is that the amount of  $\text{Fe}_3\text{B}$  precipitated is higher in the Si5 alloy than that in the Si9 alloy. It is possible that the precipitation of  $\text{Fe}_3\text{B}$  is inhibited by the higher concentration of silicon [14]. We also examined the changes in the line widths,  $\Gamma$ , of the Mössbauer lines characteristic of  $\text{Fe}_3\text{B}$  and  $\text{Fe}_2\text{B}$  phases with  $t$  (annealing time). The results for Si5 and Si9 alloys, when annealed at 475°C indicate that  $\Gamma$  decreases with  $t$  for the  $\text{Fe}_2\text{B}$  phase. This behaviour needs further examination.

Glassy alloys having high iron content can possess long-range magnetic ordering, although there is no long-range structural ordering in them. It is well known that useful information about the direction of the magnetic moments in these alloys can be obtained from the knowledge of the relative intensities of the hyperfine lines in the measured Mössbauer spectra. In the case of  $^{57}\text{Fe}$ , 14.4 keV  $\gamma$ -ray Mössbauer spectroscopy, the ratio,  $b$ , of the intensities of the second to the first hyperfine lines is given [31] by  $(4 \sin^2 \theta) / [3(1 + \cos^2 \theta)]$ , where  $\theta$  is the angle between the magnetization direction and the  $\gamma$ -ray propagation direction. The samples of the metallic glasses are usually mounted on copper holders and such clamping affects the direction of the magnetic moment in the sample. Previous studies [31] have shown that the direction of the magnetic moments in the as-received samples are affected by the strain frozen in the alloy during the rapid-quenching process. Annealing at high temperatures releases these stresses resulting in a change of the moment directions.

To investigate similar effects in the present samples, we used the areal ratios of the Mössbauer spectral lines to determine  $b$  and  $\theta$ . The present results showed that the values of  $\theta$  observed for the as-received samples of Si5 and Si9 alloys are 90° (all moments are parallel to the plane of the ribbon) and 68° (magnetization direction rotates out of the plane of the ribbon), respectively. Increase in the silicon concentration, therefore, appears to lower the  $\theta$  value. Similar metalloid dependence of the magnetic anisotropy (decreasing  $\theta$  with silicon concentration) has also been reported for other Fe–B–Si [32, 33] alloys. We also examined the effect on  $\theta$  of the temperature and time of annealing. Both metallic glasses (samples Si5 and Si9) showed that compared to the values of the as-prepared samples,  $\theta$  decreased with annealing temperature. For the fixed annealing temperature,  $\theta$  values for both the glasses decreased with the time period of annealing. Similar behaviour has been reported for other metallic glasses [31, 34–36]. The results indicate that annealing does relieve internal stresses in the sample which are invariably present in the rapidly quenched alloys. Because the direction of magnetization is stress-sensitive, this relief in the internal stress is reflected in the directional change of the magnetization axis. The effects of annealing are usually interpreted in terms of a reduction of the number of vacancies and an increase in the topological order approaching a relaxed, ideal glass.

#### 4. Conclusion

The amorphous nature of the as-received samples of  $\text{Fe}_{79}\text{B}_{16}\text{Si}_5$  and  $\text{Fe}_{78}\text{B}_{13}\text{Si}_9$  is maintained even when the glasses are heated up to 400°C for different times not exceeding 16 h.

In the case of amorphous  $\text{Fe}_{79}\text{B}_{16}\text{Si}_5$  glass the crystallization process appears to commence when the sample is heated at 450°C for 4 h or more, whereas for the  $\text{Fe}_{78}\text{B}_{13}\text{Si}_9$  samples, the crystallization process starts after heat treatment is carried out at 475°C for



1 h. Thus properties pertaining to the amorphous nature of the alloys (namely, diffusion of atomic species) should be performed for temperatures below 450 °C for Fe<sub>79</sub>B<sub>16</sub>Si<sub>5</sub> and below 475 °C for Fe<sub>78</sub>B<sub>13</sub>Si<sub>9</sub>. These properties measured on the samples heated to 475 °C for 8 h will neither belong to the amorphous phase nor to the crystalline phase, because we found that the crystallization of these glasses is not complete when heated to 475 °C for 8 h.

Upon annealing the direction of magnetization in the Fe–B–Si glasses has been observed to change its orientation.

Against this background of extensive investigation of structural changes occurring in these metallic glasses for long annealing durations below the reported crystallization temperature, the diffusion studies in these glasses, were undertaken. These investigations have helped us to identify the range of temperature and times of heat treatment which can be employed for investigating diffusion coefficients in the amorphous structure of these metallic glasses [7].

### Acknowledgement

This research was supported in part by the Council of Scientific and Industrial Research (CSIR), New Delhi, India, under the Project no. 3(689)/90-EMR-II. The financial support of the CSIR is gratefully acknowledged.

### References

1. T. MASUMOTO and K. SUZUKI (eds), "Proceedings of the 4th International Conference on Rapidly Quenched Metals" (Japan Institute of Metals, Sendai, 1982).
2. F. E. LUBORSKY (ed.), "Amorphous Metallic Alloys" (Butterworth, London, 1983).
3. R. HASEGAWA (ed.), "Glassy Metals: Magnetic, Chemical and Structural Properties" (CRC Press, FL, 1983) p. 179.
4. M. N. CHANDRASEKHARIAH, in "Metallic Glasses: Production, Properties and Applications", edited by T. R. Anantharaman, (Trans Tech, Aedermannsdorf, Switzerland, 1984) p. 269.
5. B. CANTOR and R. W. CAHN, in "Amorphous Metallic Alloys" edited by F. E. Luborsky (Butterworth, London, 1983) p. 487.
6. N. BANERJI, PhD thesis, Indian Institute of Technology, Kanpur, India (1993) unpublished.
7. N. BANERJI, V. N. KULKARNI and R. M. SINGRU, to be published.
8. Goodfellow Metals Ltd, Cambridge, UK, Catalogue (1990).
9. V. R. V. RAMANAN and G. E. FISH, *J. Appl. Phys.* **53** (1982) 2273.
10. A. ZALUSKA and H. MATYJA, *J. Mater. Sci.* **18** (1983) 2163.
11. C. F. CHANG and J. MARTI, *ibid.* **18** (1983) 2297.
12. A. QUIVY, J. RZEPSKI, J. P. CHEVALIER and Y. CALVAYRAC, in "Rapidly Quenched Metals V", edited by S. Steeb and H. Warlimont (Elsevier Science, Amsterdam, 1985) p. 315.
13. S. SURINACH, M. D. BARO and N. CLAVAGUERA, *ibid.*, p. 323.
14. T. NAGARAJAN, ASARI U. CHIDAMBARAM, S. SRINIVASAN, V. SRIDHARAN and A. NARAYANASAMY, *Mater. Sci. Eng.* **97** (1988) 355.
15. J. Y. BANG and R. Y. LEE, *J. Mater. Sci.* **26** (1991) 4961.
16. R. SINGHAL, U. C. JOHRI and R. M. SINGRU, *ibid.* **28** (1993) 975.
17. A. K. BHATNAGAR and N. RAVI, *Phys. Rev. B* **28** (1983) 359.
18. M. TANIWAKI and M. MAEDA, *Mater. Sci. Eng.* **99** (1988) 47.
19. U. GONSER, M. GHAFARI, M. ACKERMANN, H. P. KLEIN, J. BAUR and H. G. WAGNER, in "Proceedings of the 4th International Conference on Rapidly Quenched Metals", edited by T. Masumoto and K. Suzuki (Japan Institute of Metals, Sendai, 1982) p. 639.
20. L. HAGGSTROM, L. GRANAS, R. WAPPLING and S. DEVANARAYANAN, *Phys. Scripta* **7** (1973) 125.
21. F. H. SANCHEZ, Y. D. ZHANG, J. I. BUDNICK and R. HASEGAWA, *J. Appl. Phys.* **66** (1989) 1671.
22. L. TAKACS, M. C. CADEVILLE and I. VINCZE, *J. Phys. F* **5** (1975) 800.
23. G. LE CAER and J. M. DUBOIS, *Phys. Status Solidi A* **64** (1981) 275.
24. L. HAGGSTROM, L. GRANAS, R. WAPPLING and S. DEVANARAYANAN, *Phys. Scripta* **7** (1973) 125.
25. HANG NAM OK, K. S. BAEK and C. S. KIM, *Phys. Rev. B* **24** (1981) 6600.
26. T. KEMENY, I. VINCZE, R. FOGARASSY and ARAJS SIGURDS, *ibid.* **20** (1979) 476.
27. J. A. CUSIDO, A. ISALGUE and J. TEJADA, *Phys. Status Solidi A* **87** (1985) 169.
28. I. NOWIK, I. FELNERT, Y. WOLFUS and Y. YESHURUN, *J. Phys. F* **18** (1988) L 181.
29. HANG NAM OK and A. H. MORRISH, *Phys. Rev. B* **22** (1980) 3471.
30. A. K. BHATNAGAR and N. RAVI, *J. Non-Cryst. Solids* **56** (1983) 237.
31. C. L. CHIEN, *Phys. Rev. B* **18** (1978) 1003.
32. F. E. LUBORSKY, P. J. FLANDERS, H. H. LIBERMANN and J. L. WALTER, *IEEE Trans. Magn.* **MAG-15** (1979) 1961.
33. S. T. LIN, L. Y. JANG and L. S. CHOU, *Solid State Commun.* **38** (1981) 853.
34. M. W. RUCKMAN, R. A. LEVY and A. KESSLER, *J. Non-Cryst. Solids* **40** (1980) 393.
35. R. KAMAL, S. BJARMAN and R. WAPPLING, *Phys. Scripta* **23** (1981) 57.
36. A. K. BHATNAGAR, D. GANESAN, B. BHANU PRASAD, R. S. PARASHAR and R. JAGANNATHAN, in "Rapidly Quenched Metals V", edited by S. Steeb and H. Warlimont (Elsevier Science, Amsterdam, 1985) p. 295.

Received 28 September 1993  
and accepted 27 July 1994